Design and Implementation Unit Cell for 6G Reconfigurable Intelligent Surface Application

https://doi.org/10.3991/ijoe.v19i05.37585

Jaafar Qassim Kadhim(✉), Adheed H. Sallomi
Electrical Engineering Department, College of Engineering, Mustansiriyah University, Baghdad, Iraq
jaafar80@uomustansiriyah.edu.iq

Abstract—This article presents a model through which the reflection coefficient amplitude as well as phase of reflective intelligent surfaces can be estimated accurately. The reconfigurability of the surface was achieved by incorporating the varactor diodes into the surface of the cell unit. The manipulation of the phase of the reflection coefficient can be achieved by making adjustments to the biasing state of the varactors. The model, which makes use of a physics-based methodology and is based on a transmission-line circuit description of the Reconfigurable Intelligent surfaces (RIS) unit cells, considers every pertinent electrical and geometrical characteristics of the proposed surface. With the method proposed in this paper, fast and accurate RIS-based communication lines can be created. The recommended accuracy of the proposed method was confirmed through the use of a CST microwave studio full-wave simulations.

Keywords—RIS, 6G, Intelligent Surface, MIMO, CST

1 Introduction

In recent times, researchers and practitioners have proposed Reconfigurable Intelligent surfaces (RISs) as a solution to 5G communication networks due to the fact that they are capable of reflecting and deviating electromagnetic waves that come in contact with them. They are able to achieve this by adjusting the biasing state of active components that come in contact with the reconfigurable intelligent. Unlike the MIMO arrays that receive, down-convert, and retransmit the signals that come in contact with their surface, the RIS is known for providing a solution that is energy-efficient for wireless systems that may emerge in the future [1–5]. This is attributed to the ability of the RISs to provide full reflection of the incident waves towards a particular direction which could be the location of a user. Given this ability of the RIS, the RIS-assisted links do not require amplifiers and related complex microwave components [5]. For the reflected field to be focused towards a particular direction, a biasing network with the ability to regulate the reflection phase as well as the amplitude of each single element found in the RIS is needed. In normal situations, obtaining the surface's reconfigurability requires incorporating the varactor diodes into the unit cell of the surface. The control of the phase of the reflection coefficient can be achieved by distinguishing

the biasing state of the varactors. Normally, the amplitude of the reflection coefficient should be equal to one but, practically, it is less than one as a result of losses and field dissipations that occur in the process.

Despite the benefits offered by RIS-assisted wireless communications, it is accompanied by a limitation, which is the absence of accurate models that provide description of reconfigurable metasurfaces as a function of their electromagnetic properties. A large number of studies conducted till date majorly hypothesizes that the perfect control of phase and amplitude reflection is achieved by metasurfaces. In very recent works, researchers make use of empirical model that allows the inclusion of reflection losses. Sadly, this model is characterized by the absence of a connection with the physical hardware, and does not regard the reliance of the reflection coefficient on the RIS from the incidence angle as a critical aspect [6, 7].

Thus, in this work, a model that takes into consideration the specific geometry of the element including every physical parameter that are needed for the provision of an accurate design of the RIS like the periodicity of the surface, incidence angle, and mutual coupling alongside neighboring elements, varactors diodes' status, thickness and permittivity of the dielectric substrate. More so, the technique proposed in this paper takes into cognizance the interaction of the periodic surface alongside the RIS ground plane. The proposed model is completely analytical and as such, it has just little computational complexities. In order to verify the accuracy of the proposed approach, full-wave simulations were conducted using CST Microwave Studio.

2 Related work

Recently, significant research advancement has been recorded in the area of RIS [8–10]. RIS is a reflector that supports extant communication by reflecting impinging signal towards a particular direction. Through the use of RIS-supported communications, spectral and energy efficiency can be enhanced, significantly. Also, the use of RIS can lead to significant improvement in a channel's secrecy rate. Other relevant applications of RIS include non-orthogonal multiple access and cogitative radio. RIS is made up of a huge amount of unit cells, and each of them has the capability of tuning the magnitude or phase of the reflected wave. The RISs which are also cost-effective and energy-efficient, can simply be fixed on the wall of a building. RIS can be used to significantly improve signal-to-noise ratio and to suppress co-channel interference. Thus, it is possible achieve significant improvement in communication performance through the use of RIS alone without extra antennas.

In recent time, researchers have published on the hardware aspect of RIS beyond applications in 5G/6G, while many other articles have focused on techniques that can be used in measuring the performance of RIS. RISs unit cell elements can also be based on printed patches with modified shapes connected by the tuning components (varactor or PIN diodes) [11, 12], printed microstrip lines connected by the tuning components to the ground plane [13], or single printed patch element structure [14]. The authors in used two varactors to establish a connection between microstrip lines with the ground plane, and a phase shift of at least 180º at 5.8 GHz using 1-bit arrangement was recorded. Similarly, [15], using the same unit cells, were able to develop half of the structure using

one varactor diode, thereby achieving a phase tuning range over 300º around 22 GHz. The authors in [16], used a unit cell based on microstrip lines connected by a varactor diode. The authors recorded a phase shift of 180º and 120º at 5.6 GHz. In [17], the authors focused on overcoming the limitation of phase states with PIN diodes as tuning elements by combining a slot structure characterized by five PIN diodes with a top patch element at 28.5 GHz. The arrangement of the PIN diodes was done in a way that only two control signals were needed for the production of a 2-bit unit cell with four quantized near 90º increment phase states. The use of two PIN diodes was employed by the researchers in [18]; they were connected to a grounded patch, and a 2-bit unit cell at 7.25 GHz was achieved. Lastly, in the work done by [19] a PIN controlled unit cell based on patch elements with parasitic resonators at 28.5 GHz was described. The aim of the proposed approach was to minimize the loss of reflection caused by dissipation that occurred in the patch resonators shunted to the ground. Unlike in other studies, the authors in [15, 20] combined varactor with PIN diode within the same unit cell. The PIN diode was responsible for generating two-phase states with a 180º difference and a varactor equipped to support the extension of its frequency range and to achieve varying reflection phases.

3 Lumped element tuning with voltage

One of the most efficient ways to realize tunable metasurfaces, especially for microwave implementations is through the use of tunable lumped electronic elements, for which the input impedance can be tuned by means of DC voltage signals (biasing). Some examples of such characteristics include, P-N varactor diodes, variable resistors, and PIN switch diodes. In order to realize tunable metasurfaces, lumped elements can be incorporated into the metal atom configuration while using the most appropriate biasing signals to address them. The collective control of all elements through the modulation of the global bias voltage results in the uniform modification of the surface impedance of the metasurface. This in turn, can result in the tuning of preselected functionality.

3.1 Switch diodes

A PIN switch diode has two states which are “ON” (conducting) and “OFF” (insulating), and the two states can be realized through forward bias and zero- (or reverse-) bias, respectively. Through this, switchable metasurfaces with the ability to toggle between two different operating states can be enabled. For instance, the authors in study [21] proposed a metasurface that has switchable response between full reflection and total absorption by tuning the bias voltage. The diode’s state has an influence on the surface’s impedance of the metasurface to match (total absorption) or mismatch (total reflection) with the free-space impedance. Using a different design, the authors in [22] made modifications to both polarization and scattering properties. If the state of the diodes is “on”, wave that is characterized by linear polarization and is in contact with the metasurface is reflected while the same polarization is retained. Meanwhile, when the state of the diodes is “off” transmission of the incident wave occurs with perfect polarization conversion to the orthogonal state.

3.2 Varactor diodes

The P-N varactor diodes which are also referred to as tunable capacitors are also a kind of lumped elements used on metasurfaces as shown in Figure 1. The reactance of his kind of lumped elements can be modified, thereby, continuously causing slight change in resistance by varying the reverse bias voltage [23]. This is unlike what is obtainable in the two different states in switch diodes. Frequency tenability can be achieved by collectively addressing the varactors using the same voltage [24, 25]. Tunable perfect absorption is one of the functionalities that is widely and actively researched on; the modification of the reverse biasing voltage of the varactors causes the resonance frequency to shift, thereby achieving the spectral position that permits perfect absorption [26, 27]. Typically, capacitances in the order of few pico Farads (0.5–5 pF) are needed for this purpose, and can be obtained together with commercially available diodes that make use of moderate reverse bias voltages of the order of 0–15 V. More so, off-the-shelf varactors can be incorporated into GHz meatsurfaces as they can be obtained in few cubic millimeters.

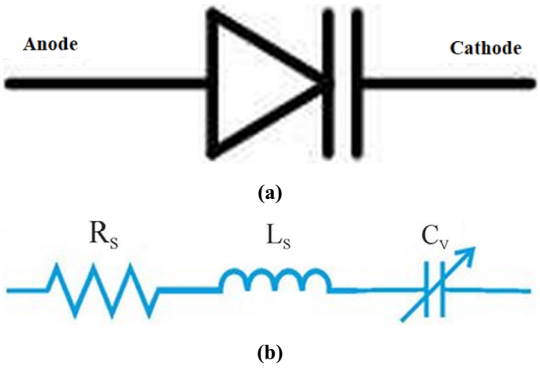

Fig. 1. It shows that (a) Varactor Diode, and (b) the equivalent circuit of Varactor Diodes

4 Proposed work

This section presents evaluation results of the unit cell designed in this study. Simulations were performed using CST studio suite software which was commercially obtained. Specifically, in CST the considered configuration is the boundary condition as unit cell in – and $\hat{x}$ $\hat{y}$-directions with open-add space in $\hat{z}$-direction. The use of frequency domain solver was employed in simulating the reflection and reflectivity phases.

Figure 2 shows the design of the unit cell of the RIS proposed in this work. The size of the unit cell is 5 mm × 5 mm. For the design of the unit cell, a Rogger 5880 substrate characterized by loss tangent of 0.0009, thickness of 0.8 mm, and dielectric constant of 2.2 was used. The base element for the RIS design was the single-element unit cell. The construction of this kind unit cell is simple, and hence, the decision to use it for the RIS design proposed in this work. In addition, the parameters values which used in the proposed work of Figure 1 (R = 1.06 Ω, L_S = 0.05 nH, and vay C to adjust the reflection phase.

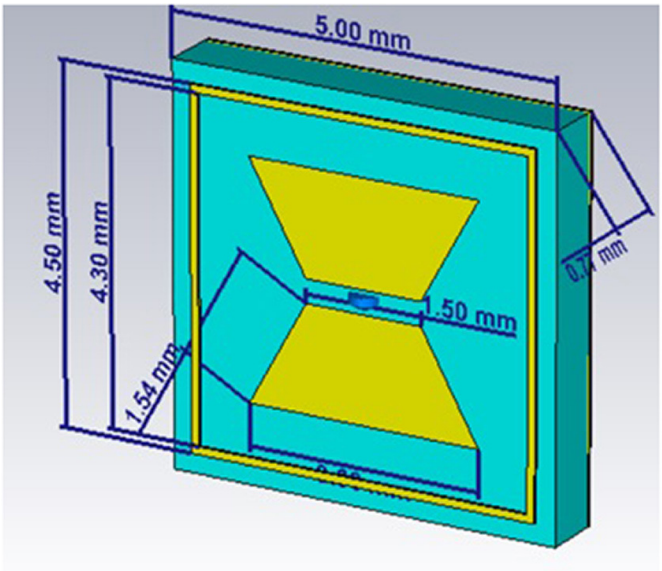

Fig. 2. The proposed unit cell

5 Result and discussion

The results for reflection phase and reflection loss parameters of the unit cells are presented in this section. The simulated reflection loss and reflection phase of the proposed unit cell are shown in Figures 3 and 4, respectively. From the reflection loss and reflection phase, it can be seen clearly that the reflection of power by the unit cells occur at a frequency band of between (18–30) GHz. Figure 3 clearly shows that change in the capacitor value occurs as a result of change in reflection. More so, a satisfactory result was achieved.

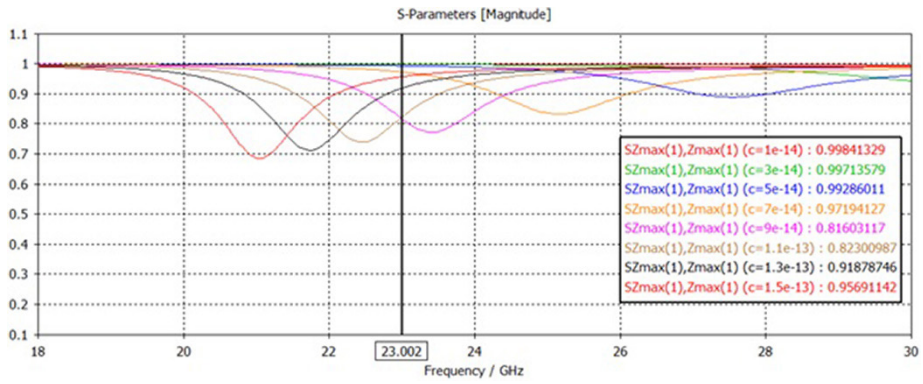

Fig. 3. Amplitude versus the frequency of the impinging signal for a unit cell that induces arg (Γc) phase shift at 23 GHz

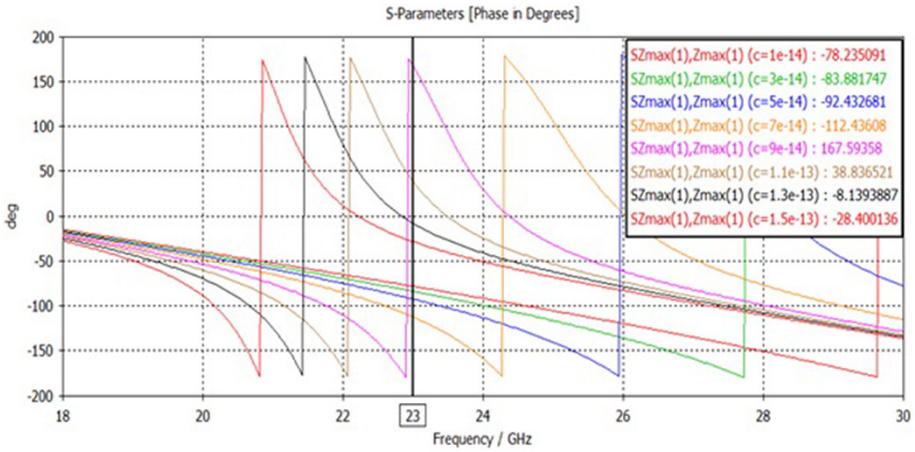

Fig. 4. Phase shift versus the frequency of the impinging signal for a unit cell that induces arg (Γc)

Also, the reaction of the RIS to wideband signal shown in Figures 3 and 4 was investigated by plotting the phase and amplitude of the unit cell's reflection coefficient against the signal frequency, respectively, where the variable capacitance is adjusted to achieve a phase shift denoted by arg (Γc). It can be clearly seen that the reaction of the RIS in terms of amplitude and phase caused by the unit cell in the direction of an impinging wave differs according to the frequency. Therefore, the RIS results in dispersion to the wideband signal given that the various frequencies produce varying reflection coefficients.

6 Conclusion

In recent times, there has been rapid advancement of the RIS technology due to the increasing demand for cost-effective and energy efficient beam forming systems. Consequently, researchers have explored a wide variety of RIS applications including, wireless coverage extension, wireless power delivery, and efficient channel estimation. The cost of producing the proposed RIS is quiet low because of its nature, which is planar and simple. With this, the deployment of large RIS can be carried out at a relatively low cost with better performance as compared to other competing technologies. The use of varactor diodes which were integrated into the surface of the unit cell was employed in the production of the reconfigurable unit cell proposed in this study. The aim of incorporating them is to achieve reconfigurability of the surface. In order to manipulate the phase of the reflection coefficient, the varactors' biasing state can be adjusted, where adjustment is made to the variable capacitance so that a phase shift which allows the derivation of a (–160 to 160) phase difference can be achieved. Future research will focus on combining unit cells to enable the conceptualization of the digital coding metasurface characterized by reconfigurable properties that enable the RIS design.

7 Acknowledgements

The authors express their gratitude to Mustansiriyah University in Iraq for supporting this study.

8 References

[1] T. Sharma, A. Chehri, and P. Fortier, "Reconfigurable intelligent surfaces for 5G and beyond wireless communications: A comprehensive survey," *Energies,* vol. 14, no. 24, p. 8219, 2021. https://doi.org/10.3390/en14248219

[2] R. Liu, G. C. Alexandropoulos, Q. Wu, M. Jian, and Y. Liu, "How can reconfigurable intelligent surfaces drive 5G-advanced wireless networks: A standardization perspective," in *2022 IEEE/CIC International Conference on Communications in China (ICCC Workshops)*, 2022: IEEE, pp. 221–226. https://doi.org/10.1109/ICCCWorkshops55477.2022.9896658

[3] J. Chen, S. Wang, J. Jia, Q. Wang, L. Yang, and X. Wang, "Multi-objective oriented resource allocation reconfigurable intelligent surface assisted HCNs," *Ad Hoc Networks,* p. 103066, 2022. https://doi.org/10.1016/j.adhoc.2022.103066

[4] H. T. S. AlRikabi, A. H. M. Alaidi, A. S. Abdalrada, and F. T. Abed, "Analysis of the efficient energy prediction for 5G wireless communication technologies," *International Journal of Emerging Technologies in Learning,* vol. 14, no. 8, pp. 23–37, 2019. https://doi.org/10.3991/ijet.v14i08.10485

[5] E. Basar, M. Di Renzo, J. De Rosny, M. Debbah, M.-S. Alouini, and R. Zhang, "Wireless communications through reconfigurable intelligent surfaces," *IEEE Access,* vol. 7, pp. 116753–116773, 2019. https://doi.org/10.1109/ACCESS.2019.2935192

[6] E. Björnson, Ö. Özdogan, and E. G. Larsson, "Reconfigurable intelligent surfaces: Three myths and two critical questions," *IEEE Communications Magazine,* vol. 58, no. 12, pp. 90–96, 2020. https://doi.org/10.1109/MCOM.001.2000407

[7] J. P. Turpin, J. A. Bossard, K. L. Morgan, D. H. Werner, and P. L. Werner, "Reconfigurable and tunable metamaterials: A review of the theory and applications," *International Journal of Antennas and Propagation,* vol. 2014, Article ID 429837, 2014. https://doi.org/10.1155/2014/429837

[8] W. Tang *et al.*, "Wireless communications with reconfigurable intelligent surface: Path loss modeling and experimental measurement," *IEEE Transactions on Wireless Communications,* vol. 20, no. 1, pp. 421–439, 2020. https://doi.org/10.1109/TWC.2020.3024887

[9] Y. Liu *et al.*, "Reconfigurable intelligent surfaces: Principles and opportunities," *IEEE Communications Surveys & Tutorials,* vol. 23, no. 3, pp. 1546–1577, 2021. https://doi.org/10.1109/COMST.2021.3077737

[10] W. Tang *et al.*, "MIMO transmission through reconfigurable intelligent surface: System design, analysis, and implementation," *IEEE Journal on Selected Areas in Communications,* vol. 38, no. 11, pp. 2683–2699, 2020. https://doi.org/10.1109/JSAC.2020.3007055

[11] J. Wang *et al.*, "Reconfigurable intelligent surface: Power consumption modeling and practical measurement validation," *arXiv preprint arXiv:2211.00323,* 2022.

[12] K. Mensah-Bonsu, B. Yang, A. Eroglu, H. Xu, and L. Qian, "Equivalent circuit model for varactor-loaded reconfigurable intelligent surfaces," in *2022 IEEE International Symposium on Antennas and Propagation and USNC-URSI Radio Science Meeting (AP-S/URSI)*, 2022: IEEE, pp. 1190–1191. https://doi.org/10.1109/AP-S/USNC-URSI47032.2022.9887171

[13] L. G. da Silva, P. Xiao, and A. Cerqueira, "A 2-bit tunable unit cell for 6G reconfigurable intelligent surface application," in *2022 16th European Conference on Antennas and Propagation (EuCAP)*, 2022: IEEE, pp. 1–5. https://doi.org/10.23919/EuCAP53622.2022.9769482

[14] K. Kaboutari and V. Hosseini, "A compact 4-element printed planar MIMO antenna system with isolation enhancement for ISM band operation," *AEU-International Journal of Electronics and Communications,* vol. 134, p. 153687, 2021. https://doi.org/10.1016/j.aeue.2021.153687

[15] C. Huang, C. Zhang, J. Yang, B. Sun, B. Zhao, and X. Luo, "Reconfigurable metasurface for multifunctional control of electromagnetic waves," *Advanced Optical Materials,* vol. 5, no. 22, p. 1700485, 2017. https://doi.org/10.1002/adom.201700485

[16] W. Li *et al.*, "Programmable coding metasurface reflector for reconfigurable multibeam antenna application," *IEEE Transactions on Antennas and Propagation,* vol. 69, no. 1, pp. 296–301, 2020. https://doi.org/10.1109/TAP.2020.3010801

[17] L. Dai *et al.*, "Reconfigurable intelligent surface-based wireless communications: Antenna design, prototyping, and experimental results," *IEEE Access,* vol. 8, pp. 45913–45923, 2020. https://doi.org/10.1109/ACCESS.2020.2977772

[18] C. Huang, B. Sun, W. Pan, J. Cui, X. Wu, and X. Luo, "Dynamical beam manipulation based on 2-bit digitally-controlled coding metasurface," *Scientific Reports,* vol. 7, no. 1, pp. 1–8, 2017. https://doi.org/10.1038/srep42302

[19] J.-B. Gros, V. Popov, M. A. Odit, V. Lenets, and G. Lerosey, "A reconfigurable intelligent surface at mmWave based on a binary phase tunable metasurface," *IEEE Open Journal of the Communications Society,* vol. 2, pp. 1055–1064, 2021. https://doi.org/10.1109/OJCOMS.2021.3076271

[20] A. Roy, Y. Naresh, A. Padmanabhan, A. Chockalingam, and K. Vinoy, "Digitally reconfigurable metasurface array for a multipath based wireless link with media-based modulation," *IEEE Transactions on Microwave Theory and Techniques,* vol. 70, no. 12, pp. 5418–5426, 2022. https://doi.org/10.1109/TMTT.2022.3207988

[21] B. Zhu, Y. Feng, J. Zhao, C. Huang, and T. Jiang, "Switchable metamaterial reflector/absorber for different polarized electromagnetic waves," *Applied Physics Letters,* vol. 97, no. 5, p. 051906, 2010. https://doi.org/10.1063/1.3477960

[22] Z. Tao, X. Wan, B. C. Pan, and T. J. Cui, "Reconfigurable conversions of reflection, transmission, and polarization states using active metasurface," *Applied Physics Letters,* vol. 110, no. 12, p. 121901, 2017. https://doi.org/10.1063/1.4979033

[23] J. Zhao, Q. Cheng, J. Chen, M. Q. Qi, W. X. Jiang, and T. J. Cui, "A tunable metamaterial absorber using varactor diodes," *New Journal of Physics,* vol. 15, no. 4, p. 043049, 2013. https://doi.org/10.1088/1367-2630/15/4/043049

[24] C. Mias and J. H. Yap, "A varactor-tunable high impedance surface with a resistive-lumped-element biasing grid," *IEEE Transactions on Antennas and Propagation,* vol. 55, no. 7, pp. 1955–1962, 2007. https://doi.org/10.1109/TAP.2007.900228

[25] S. Burokur, J.-P. Daniel, P. Ratajczak, and A. De Lustrac, "Tunable bilayered metasurface for frequency reconfigurable directive emissions," *Applied Physics Letters,* vol. 97, no. 6, p. 064101, 2010. https://doi.org/10.1063/1.3478214

[26] Z. Luo, J. Long, X. Chen, and D. Sievenpiper, "Electrically tunable metasurface absorber based on dissipating behavior of embedded varactors," *Applied Physics Letters,* vol. 109, no. 7, p. 071107, 2016. https://doi.org/10.1063/1.4961367

[27] H. K. Kim, D. Lee, and S. Lim, "Frequency-tunable metamaterial absorber using a varactor-loaded fishnet-like resonator," *Applied Optics,* vol. 55, no. 15, pp. 4113–4118, 2016. https://doi.org/10.1364/AO.55.004113

9 Authors

Jaafar Qassim Kadhim, Electrical Engineering Department, College of Engineering, Mustansiriyah University, Baghdad, Iraq.

Adheed H. Sallomi, Electrical Engineering Department, College of Engineering, Mustansiriyah University, Baghdad, Iraq.

Article submitted 2022-11-16. Resubmitted 2023-01-14. Final acceptance 2023-01-24. Final version published as submitted by the authors.